Atomization in the acoustic field of a Hartmann whistle

S. Narayanan, K. Srinivasan* and T. Sundararajan

Department of Mechanical Engineering, Indian Institute of Technology Madras
Chennai – 600036, India

[Received date August 31, 2012; Revised version received on November 24, 2012; Accepted date: January 01, 2013]

ABSTRACT

The current work experimentally investigates the effect of Hartmann cavity acoustics on the atomization of droplet sprays. Initially, the experiments are conducted on a single droplet to understand its behavior in the sound field of a Hartmann whistle. The atomization studies on single droplet reveal that the existence of sound field causes the droplet to undergo large deformation and become irregular in shape. The degree of droplet deformation is quantified based on smaller circularity and larger Feret's diameter. The increase in cone angle of spray to a higher value in the presence of acoustics in comparison to its absence shows that the acoustics enhances the atomization. The stroboscopic visualization of sprays in the presence of acoustics further reveals the breakup of ligaments, large scatter as well as the formation of more number of droplets, indicating atomization enhancement.

Keywords: Droplet and Sprays; Hartmann whistle; Atomization applications.

NOMENCLATURE

ALR	Air to liquid ratio
C_r	Circularity
D	Spray jet diameter, m
D_c	Cavity diameter, m
D_j	Diameter of jet, m
f	Fundamental frequency of Hartmann whistle, Hz
f_s	Sampling frequency, Hz
I	Acoustic intensity, W/m^2
L	Cavity length, m
$\dot{m}_a$	Mass flow rate of air, kg/s

*Corresponding author: Tel.: +91 44 2257 4703; fax: +91 44 2257 4652, email address: ksri@iitm.ac.in (K. Srinivasan)

$\dot{m}_w$	Mass flow rate of water, kg/s
P_o	Stagnation pressure, bar
P_a	Ambient pressure, bar
R	Nozzle pressure ratio (P_o/P_a)
Re_D	Reynolds Number
S	Stand-off distance, m
SIL	Sound Intensity Level, dB
SPL	Sound Pressure Level, dB
μ_w	Dynamic viscosity of water, Ns/m^2
μ_a	Dynamic viscosity of air, Ns/m^2
μ_{mix}	Mass weighted average of the dynamic viscosity, Ns/m^2

1. INTRODUCTION

It is prominent that the introduction of sound energy into any injection system could enhance the atomization of liquid fuel. The sound field not only improves the extent of atomization but also promotes molecular agitation and turbulence. For combustion applications, aerodynamic acoustic generators like Hartmann whistle are preferred when compared to other types, since air is essential for combustion, and can also be used for sound generation. Hartmann whistle is an acoustic device wherein, jet strikes at the front end of a cylindrical cavity which is closed at the rear end. The acoustic field generated by this device can have numerous applications such as ignition, mixing, flow control etc. The present work focuses in understanding the behavior of droplets and sprays when subjected to the large and directed acoustic field of a Hartmann whistle. Some of the relevant literature on the effect of acoustics on droplets and sprays are given below.

Atomization was found to be influenced by the nature of acoustic field, in terms of position with respect to standing wave amplitude, frequency of the acoustic wave, its amplitude, and so on. Danilov and Mironov [1] traced the evolution of a small droplet in a strong acoustic field. It includes various changes in the shape of the droplets such as droplets flattening, formation of small disturbances at edge of the droplets as well as the growth of capillary waves on its surface. The instability rates and its relation with sound pressure level, frequency as well as the various parameters of the droplet were also determined. Saito *et al.* [2] studied the effect of the position of the standing wave on the evaporation or combustion rate coefficients of a single fuel droplet. At the node position, the positive effect of the acoustic wave was observed to occur under frequencies < 100 Hz and sound pressure levels > 100 dB. The acoustically disturbed rate coefficients were observed to increase two to three times higher than that of the undisturbed rate coefficients. It was also noticed that the oscillation of the surrounding gas due to the sound wave enhances mixing. Sujith *et al.* [3] theoretically studied the effect of acoustic field on the behavior of small droplets. They observed that the acoustic field can augment the heat and mass transfer to and from the droplets due to the relative motion between droplets and the gas phase. It was observed that high acoustic frequencies and large diameters lessen the droplets ability to pursue the gas phase oscillations. Murray and Heister [4] simulated the transient nonlinear response of a liquid droplet using boundary element methods when subjected to an acoustic excitation. The study discussed the effect of acoustic intensity, frequency and gas or liquid density on the behavior of droplet. At higher acoustic intensities numerous types of droplet atomization were observed. Droplet responses were observed to increase with increase of gas density. For frequencies near the second and fourth mode harmonics, enhanced droplet responses were observed.

The possibility of combustion applications of atomization added impetus to this field of research. Saito *et al*. [5] investigated the influence of acoustic field on the evaporation or combustion characteristics of a single fuel droplet by using a standing wave. The acoustic oscillation was observed to promote mixing between fuel and gas, thereby augmenting the heat and mass transfer to and from the burning droplet thus resulting an increase of combustion rate coefficient. Khandwawala *et al*. [6] experimentally investigated the use of Hartmann acoustic generator for the atomization of various fuels and observed that the extent of fuel atomization was highly sensitive to the pressure variation than the variation in the acoustic frequency. They also found that the atomization of fuel primarily depends on its surface tension and density. It was also noticed that the atomization is almost independent of the viscosity of the fuel. Swamy *et al*. [7] used the acoustic burner working on the principle of Hartmann resonator in order to understand the atomization features of high viscous fuels. The Sauter mean diameter of the fuel droplets were determined by varying the oil pressure of the fuel, atomization pressure, and air/fuel ratio. It was observed that the average sizes of droplet varied between 12 and 60 μm in comparison to the earlier works where the sizes of droplet varied from 55 to 90 μm. Dubey *et al*. [8] studied the effect of sound field on the combustion characteristics of an ethanol spray flame in a propane fired pulse combustor. It was observed that the Sauter - mean diameter of the ethanol spray reduced due to the existence of acoustic field by 15%. McQuay *et al*. [9] studied experimentally the influence of the acoustic frequency, sound pressure level, excess air and atomization of spray on NO and CO emissions from a spray flame in a Rijke tube combustor. They noticed that the presence of acoustic oscillations causes a large reduction in NO and CO emissions.

The effect of liquid properties on the atomization and ultrasonic atomization were the other areas explored. Wilcox and Tate [10] studied the atomization of liquid in a high intensity acoustic field. They measured droplet sizes for sound intensities up to 160 dB at various combinations of air and liquid flow rates. They observed that at low liquid flow rates the atomization was good whereas it became coarse at higher liquid flow rates. They also observed that the droplets were not uniformly distributed. Sujith [11] used particle image velocimetry (PIV) to characterize the spray velocity field and observed that a high intensity acoustic field (160 dB) can reduce the spray length. It was noticed that the presence of small droplets clearly illustrates that the spay velocities are reduced due to acoustic oscillations. Spray cone angle was also observed to increase due to the presence of acoustic oscillations. In addition to that the acoustic oscillations enhance the air entrainment into the spray. Barreras *et al*. [12] experimentally studied the ultrasonic atomization of water when excited with high frequency (~ MHz) waves. They observed the temporal evolution of the atomization process by depositing the liquid over an ultrasonic transducer. It was observed that ultrasonic atomization is an effective way of producing droplets of small sizes.

Acoustic field was also used for disintegrating liquid sheets, spray generation, particle agglomeration, etc. Sivadas *et al*. [13] studied the disintegration features of air-assisted liquid sheets of water due to the impact of acoustics. It was observed from the high speed photography that the optimum frequency modulation of the perturbation generator has a noticeable effect on the associated surface waves and the following breakup of the liquid sheet. The critical wave amplitude, breakup frequency and length obtained with and without acoustic excitation were compared for Weber numbers (We) varying from 0.30 to 0.44. Ju *et al*. [14] studied effect of atomization using a newly developed high frequency surface acoustic wave atomizers. The resonance frequencies were varied from 50–95 MHz. The speed of atomization and deposited dry particle diameter distribution were used to characterize the atomization. The mean diameters of the atomized droplets obtained from the dry particle diameter distribution were 5.7, 4.4 and 2.7 micrometers at frequencies of 50, 75 and 95 MHz. Shuster *et al*. [15] experimentally studied the agglomeration of submicrometer particles in acoustic field. They observed the rapid agglomeration of aerosol particles in weak periodic shock waves. It was also observed that the particle agglomeration rate was much faster in shock waves than in continuous sound waves.

1.1. Objectives of the present work

Thus, a brief review of the relevant literature reveals that although several researchers have studied the atomization of droplet and sprays in the acoustic field of different acoustic sources but negligible attempt was carried out to study the effect of acoustics on the atomization of droplet/sprays in the large and directed sound field of Hartmann whistle. The objectives are detailed below:

(i) Determination of the maximum acoustic intensity location after mapping the acoustic field of Hartmann whistle.
(ii) Initially, tuft experiments were conducted to show that the flow effects are almost absent at those injection locations of droplet and spray.
(iii) Visualization of droplet/sprays falling in the large and directed acoustic field are carried out using a high speed digital camera at 5000 frames per second.

Following the flow visualization, image analysis are carried out to understand and predict the effect of large and directed sound field of Hartmann whistle on the atomization of droplet and sprays. The current work emphasizes the fact that the large and directed sound field of Hartmann whistle could provide better mixing for various combustion processes as well as propulsion applications. The following section describes the test setup used for atomization.

2. EXPERIMENTAL SETUP

The schematic of the experimental test set-up (droplet/spray generator and Hartmann whistle) inside the anechoic chamber is shown in Fig. 1 (a). A sonic underexpanded jet emanating from a convergent nozzle of 7 mm exit diameter, attached at the end of a settling chamber, is used to impinge upon the Hartmann cavity of the same inlet

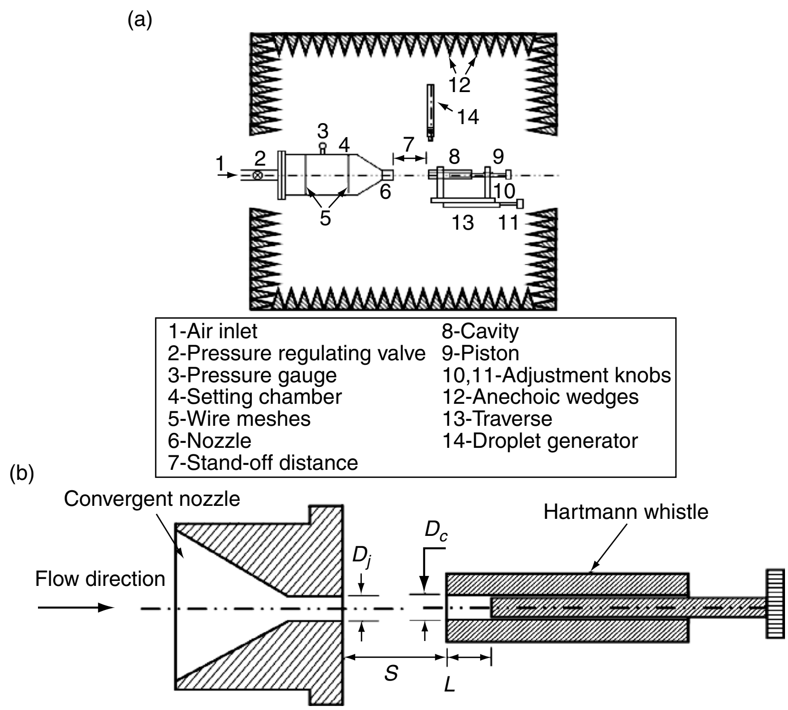

Figure 1: (a) Schematic of the experimental setup (droplet generator and Hartmann whistle facility) inside the anechoic chamber, (b) A schematic showing the parametric space (L, S, D_j, D_c) of the Hartmann whistle facility.

diameter. The length of the cavity is varied by an adjustable air tight piston capable of gliding inside the cavity. In order to vary the stand-off distance with respect to the jet flow the entire whistle facility is mounted on a linear traverse. There is provision for height adjustment in the whistle facility in order to align it correctly with respect to jet flow. The cavity length, stand-off distance and nozzle pressure ratio are the relevant parameters of the current work. The nozzle exit diameter and the inlet diameter of the cavity is maintained constant (7 mm) for the entire set of experiments. A schematic showing the parametric space (L, S, D_j, D_c) of the Hartmann whistle facility is shown in Fig. 1 (b).

Acoustic measurements are made by a 1/4” (6.35 mm diameter) condenser microphone (PCB, Model no. 377A01). The microphone data is acquired for one second at a sampling frequency (f_s) of 150 kHz and is low-pass filtered at 70 kHz, using an analog filter (Krohn- Hite, Model-3364) in order to purge aliasing errors. An angular traverse was used for mapping the acoustic field in the axial plane of the jet flow. The angular traverse moves the microphone in steps of 2° at a fixed radius of around $64D_j$ in the vertical plane and acquires data at each location and is stored on the computer. The data acquisition and motion control are simultaneously controlled by a LABVIEW program. The detailed characterization of the acoustic field was already reported by Narayanan *et al*. [16], which clearly provides the ranges of *SPL* and frequencies for the conditions of operation of the whistle.

The droplet generator test setup is shown in Fig. 2 (a). The droplets of various sizes are generated by burettes of different tip diameters. The open end of the burette is directly connected to a water tank. The location of droplets injection in a highly intense and directed sound field is varied by using a linear traverse. The single droplets are generated by adjusting the flow control knob provided in the droplet generator test-setup. The schematic of the spray atomizer is shown in Fig. 2 (b). The spray atomizer used is of effervescent type that injects air directly into the bulk liquid at some point upstream of the nozzle. The air is injected at low velocity and hence, it forms bubbles that produce a two-phase bubbly flow at the exit of the nozzle. When the air bubbles emerge from the nozzle, they undergo sudden expansion and thus break the surrounding liquid into droplets. In effervescent atomizer internal mixing is employed, i.e., the collision between the atomizing gas and the liquid occur within the atomizer body. The effervescent atomizer can provide very good atomization even at low injection pressures and air flow rates. The air flow rate and water flow rate are measured by the corresponding calibrated flow meters and they are maintained constant for a set of experiments.

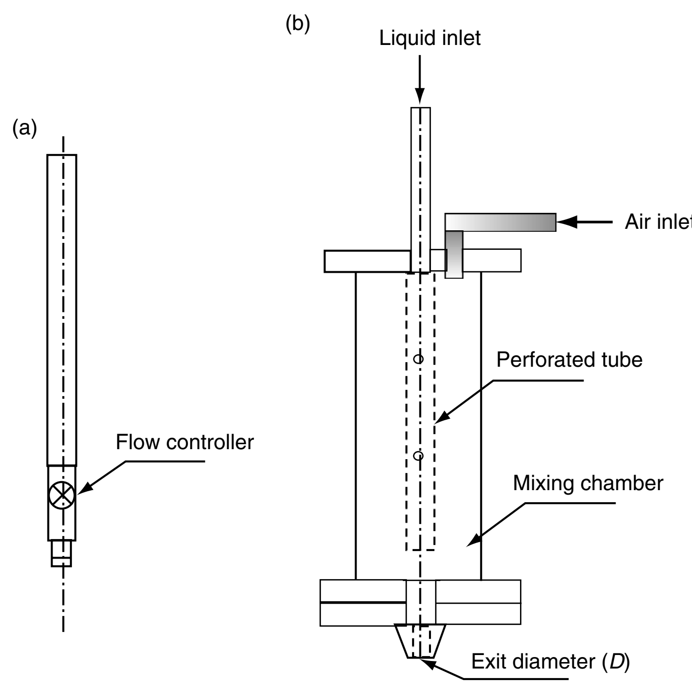

Figure 2: Schematic of (a) Droplet generator, (b) Effervescent atomizer.

The images of droplets and sprays moving through the acoustic field of Hartmann whistle are acquired using a high speed digital camera (Mikrotron Model no 1302 CMOS type). The camera has a resolution of 96 × 100 pixels and capable of capturing the images around 5000 frames per second (*fps*). A zoom lens is attached to the camera to obtain sufficient spatial resolution to accurately determine the droplet oscillation, its shape distortion as well as the cone angle variation of sprays. Tests are conducted with and without acoustic field acting on the droplets/sprays. Halogen lamps with 1000 W and 500 W are used as the source of illumination.

3. UNCERTAINTY ESTIMATES

The variation in the stagnation pressure measurement was ± 2%. The uncertainty in positioning and length of the cavity measurement was within ± 0.02 mm. The acoustic pressure measurement was varied within ± 1 dB including repeatability factors. The frequency resolution of the spectrum was 36.62 Hz.

4. ATOMIZATION STUDIES

4.1. Effect of acoustics on a single droplet

Initially, studies on single droplets are undertaken. The objective here is to explore the effect of acoustic radiation on single droplets. In order to isolate the effect of acoustics and eliminate hydrodynamic effects, tuft visualization is carried out to ensure the absence of flow at those regions of investigation. Images of tufts are taken using a high speed digital camera at 5000 *fps* for 3 s at locations of droplet injection. Water droplets are generated, and the effect of Hartmann cavity acoustics on droplets is studied for various cases.

The raw droplet image sequences with acoustics for various cavity parametric conditions R = 4.92, S/D_j = 4.57 and L/D_j = 4.28 are compared without acoustics for same time instances are shown in Fig. 3. Visual observation reveals that the droplets subjected to the acoustic field of Hartmann cavity undergoes large deformation of shape whereas no significant variation in the shape is observed on the droplets in the absence of acoustic field (Fig. 3).

The raw droplet images cannot quantify the variation in shape of the droplet due to the action of acoustics. Therefore the droplet image sequences are averaged using an image analyzer "XIMAGER" (developed at IIT Madras in the department of Aerospace Engineering and is available in the public domain (http://www.ae.iitm.ac.in/~sujith/ximager/)) in order to quantify the effect of acoustics on droplets. The analysis is done on averaged images using an image analyzer "IMAGE J". It is a public domain image analysis program developed by the National Institutes of Health (http://rsb.info.nih.gov/ij/). The effect of acoustics on the droplet is quantified by determining the parameters (i) Circularity (C_r), and (ii) Feret's diameter. The circularity (C_r) is given by the expression.

$$C_r = 4\pi \left(\frac{Area}{Perimeter^2} \right) \tag{1}$$

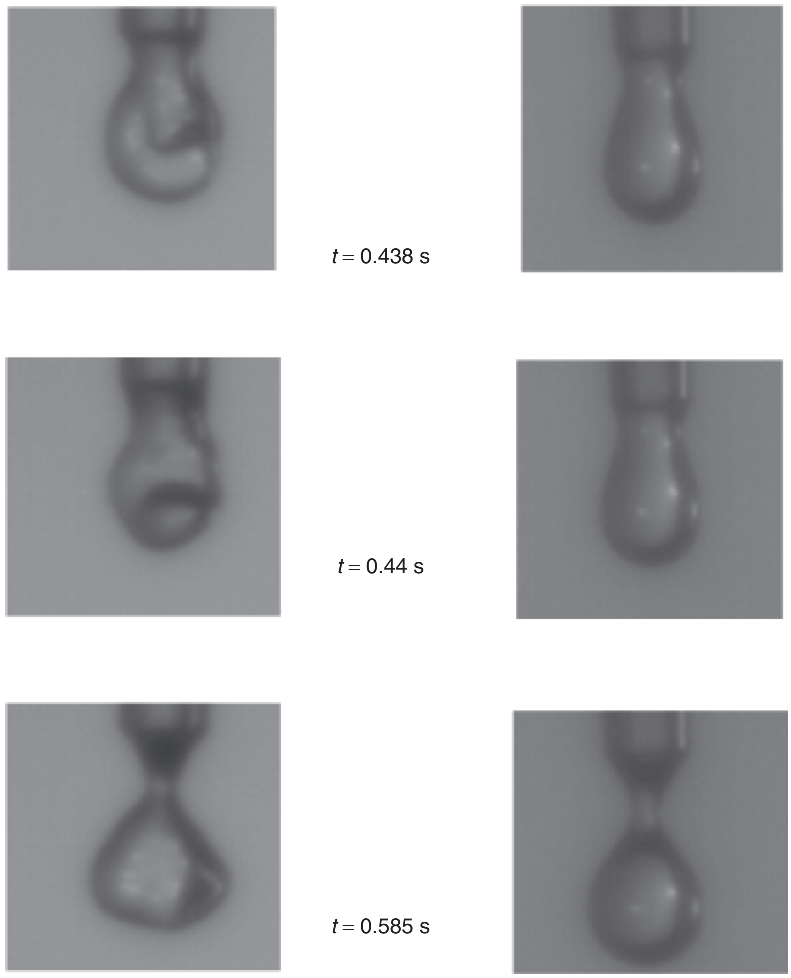

Figure 3: Droplet images with acoustics ($R = 4.92$, $S/D_j = 4.57$ and $L/D_j = 4.28$) and without acoustics are compared.

For a perfect circle, $C_r = 1$, and for an ellipse with major axis (a) and minor axis (b), $C_r = \left(\frac{2ab}{a^2 + b^2}\right)$. Feret's diameter is defined as the longest distance between any two points measured along the selection boundary.

The tip of the droplet generator used has a diameter of around 3 mm. The time-averaged images of droplets with and without acoustic interactions for various S/D_j values are shown in Figs. 4 and 5.

The presence of acoustic field causes the droplet to deform and become irregular in shape. For better visualization, the binary images of the averaged raw images are also

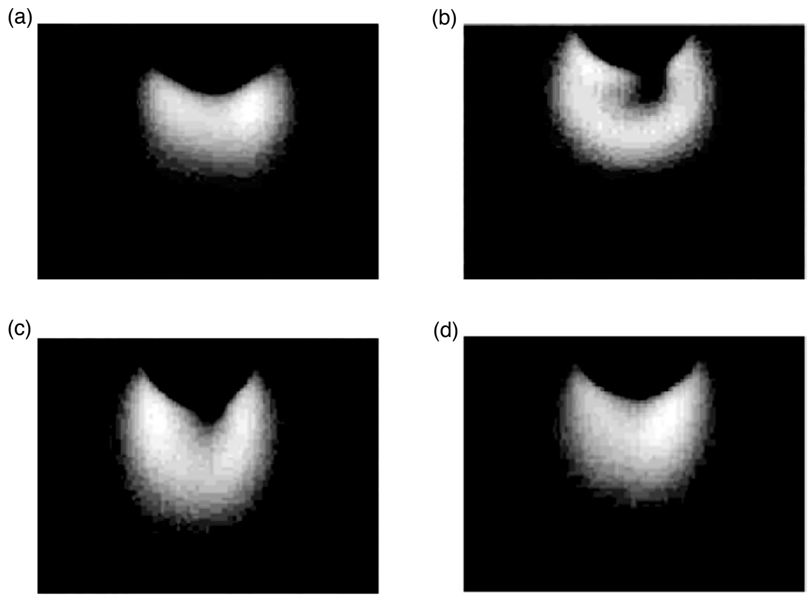

Figure 4: Average image of droplets, (a) without acoustics, (b,c,d) with acoustics at L/D_j = 4.28, R = 4.92 and S/D_j values of 2.86, 3.28 and 4.

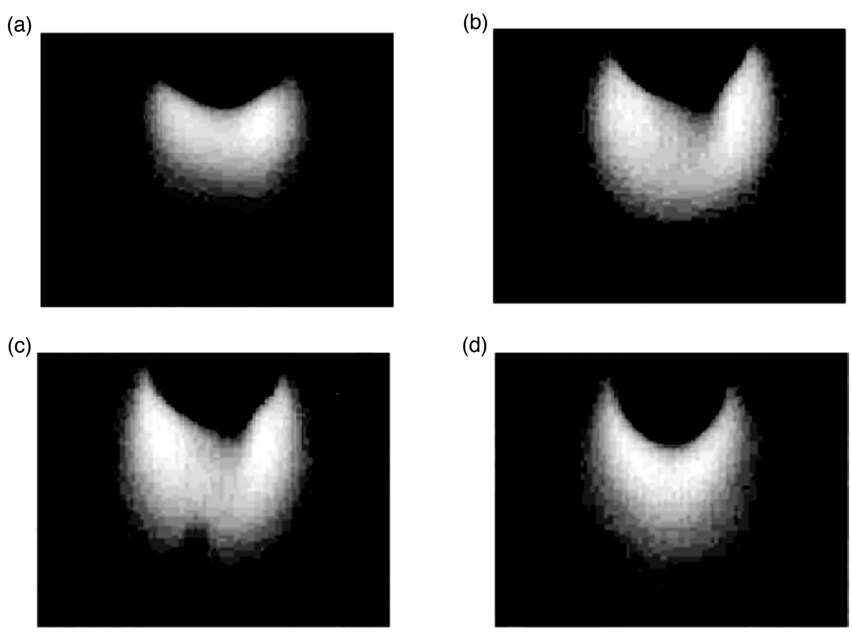

Figure 5: Average image of droplets, (a) without acoustics, (b,c,d) with acoustics at L/D_j = 4.28, R = 5.91 and S/D_j values of 2.86, 3.28 and 4.

shown in Figs. 6 and 7 at R values of 4.92 and 5.91. In binary image estimation, a constant grayscale threshold value of 128 was used for all the images.

The frequency of the acoustic field causes the droplet to undergo oscillations and the large and directed acoustic intensity causes the droplet to deform and change of shape. For injection locations, closer to the acoustic source (i.e, whistle) the acoustic intensity attains a high value, which causes large deformation of the droplets or large scatter of sprays. For locations, far-off from the acoustic source the acoustic intensity becomes weaker and thus it provides less deformation for droplets and less scatter for sprays. For both the cases mentioned above, the effect of frequency causes droplets/sprays to undergo oscillations irrespective of the locations. Thus it can be said that the acoustic intensity play a significant role for large deformation of droplets or large scatter of sprays. In the present study the droplets are injected at locations closer to the acoustic source where the acoustic intensity is high thus giving rise to large deformations in the shape of the droplet. The extent of droplet deformation is quantified based on circularity and Feret's diameter for various conditions of acoustic excitations.

The variation of circularity and Feret's diameter of the binary image of the droplet with S/D_j are shown in Fig. 8 for R values of 4.92 and 5.91. It is observed that the circularity (Fig. 8 (a)) follows an oscillatory behavior with S/D_j for both the values of R.

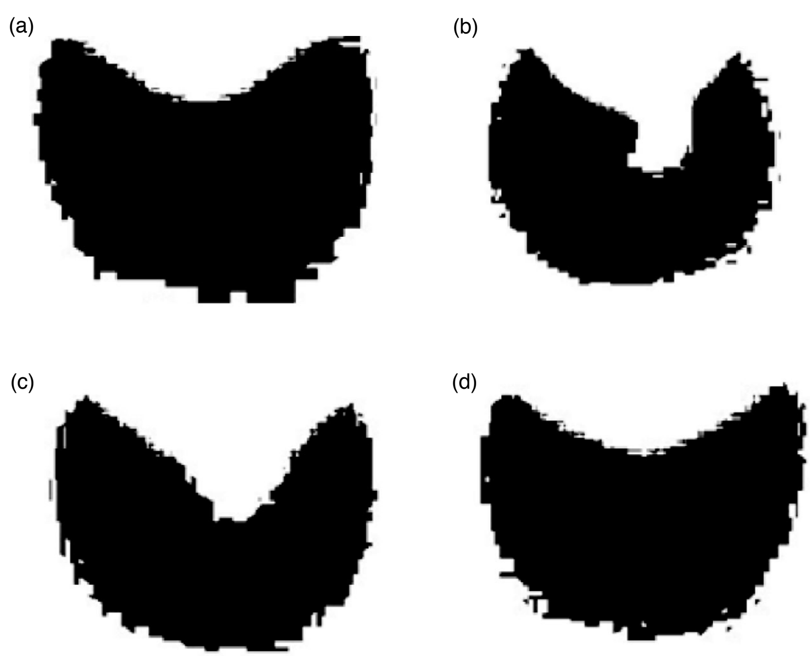

Figure 6: Binary images of averaged raw images of droplets, (a) without acoustics, (b,c,d) with acoustics at L/D_j = 4.28, R = 4.92 and S/D_j values of 2.86, 3.28 and 4.

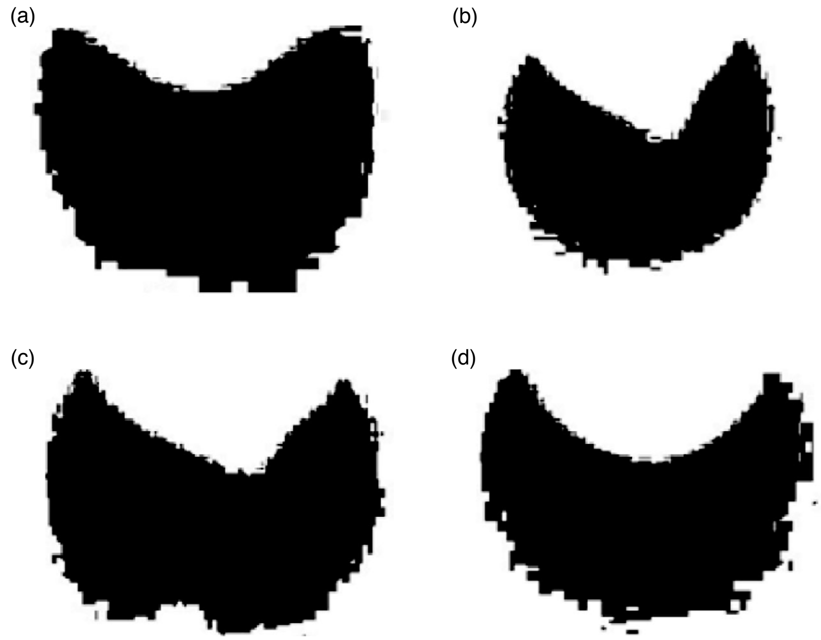

Figure 7: Binary images of averaged raw images of droplets, (a) without acoustics, (b,c,d) with acoustics at L/D_j = 4.28, R = 5.91 and S/D_j values of 2.86, 3.28 and 4.

The values of circularity observed are less at small S/D_j values for both the values of R. Also it is noticed that Feret's diameter (Fig. 8 (b)) attains maximum at smaller S/D_j values for both the values of R. Smaller circularity and large Feret's diameter at small S/D_j values indicate that the surface of the droplets becomes irregular, distorted and increasingly elongated due to impact of the acoustic oscillations.

The variation of circularity and Feret's diameter of the binary image of the droplet with fundamental acoustic frequency (f) and acoustic intensity (I) is shown in Fig. 9 at R = 4.92. The circularity as marked in Figs. 9 (a) and (b) is observed to attain minimum at f = 1978 Hz and I = 664.77 W/m^2. Feret's diameter as marked in Figs. 9 (c) and (d) becomes maximum at the same frequency and intensity.

The variation of circularity and Feret's diameter of the droplet with f and I at a higher R value of 5.91 is shown in Fig. 10. The minimum value of circularity as well as maximum value of Feret's diameter are noticed here at f = 2161 Hz and I = 537.09 W/m^2. The smaller circularity and larger Feret's diameter observed at both the R values of 4.92 and 5.91, clearly illustrate that the acoustic excitation causes the shape of droplet to be deformed from its near-spherical shape. It is however noted that gravity plays a role in these studies, wherein even unexcited droplets would assume a tear-drop shape and not a perfect spherical shape. For clarity, the circularity and Feret's diameter of unexcited droplets are shown in Figs. 9 and 10.

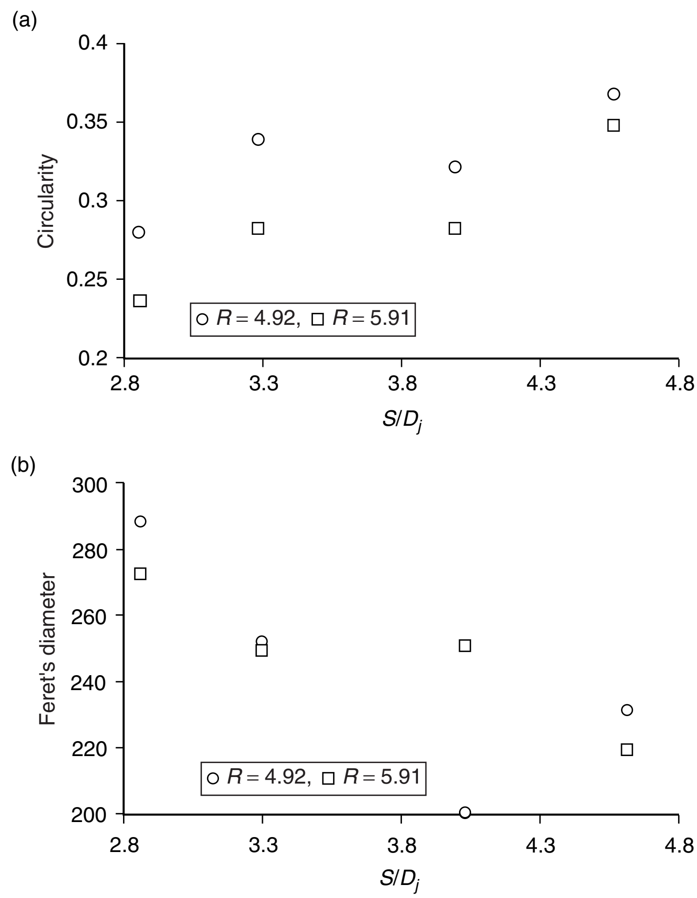

Figure 8: Variation of (a) Circularity, (b) Feret's diameter of the droplet with S/D_j at $L/D_j = 4.28$ for R values of 4.92 and 5.91.

4.2. Effect of acoustics on sprays

Similar to single droplet studies, the effect of Hartmann cavity acoustics on sprays are investigated in this section. This study is to understand the behavior of sprays in the large and directed sound field of a Hartmann whistle. The sprays generated from an effervescent atomizer with various air to liquid mass-flow-rate-ratios (ALR). The various ALR expressed in percentage are, 0.67, 1.35, 1.54, 2.06 and 2.66. These ALR are so chosen that the spray oscillations in the absence of acoustics are less. The image sequences were captured for 3 s duration at 5000 *fps*.

The instantaneous images and the corresponding edge detected images of spray in the presence of acoustics at $S/D_j = 2.86$, $L/D_j = 4.28$, $R = 5.91$ at an ALR of 0.67% is shown in Fig. 11. The image sequences of sprays reveal that the spray cone angle varies

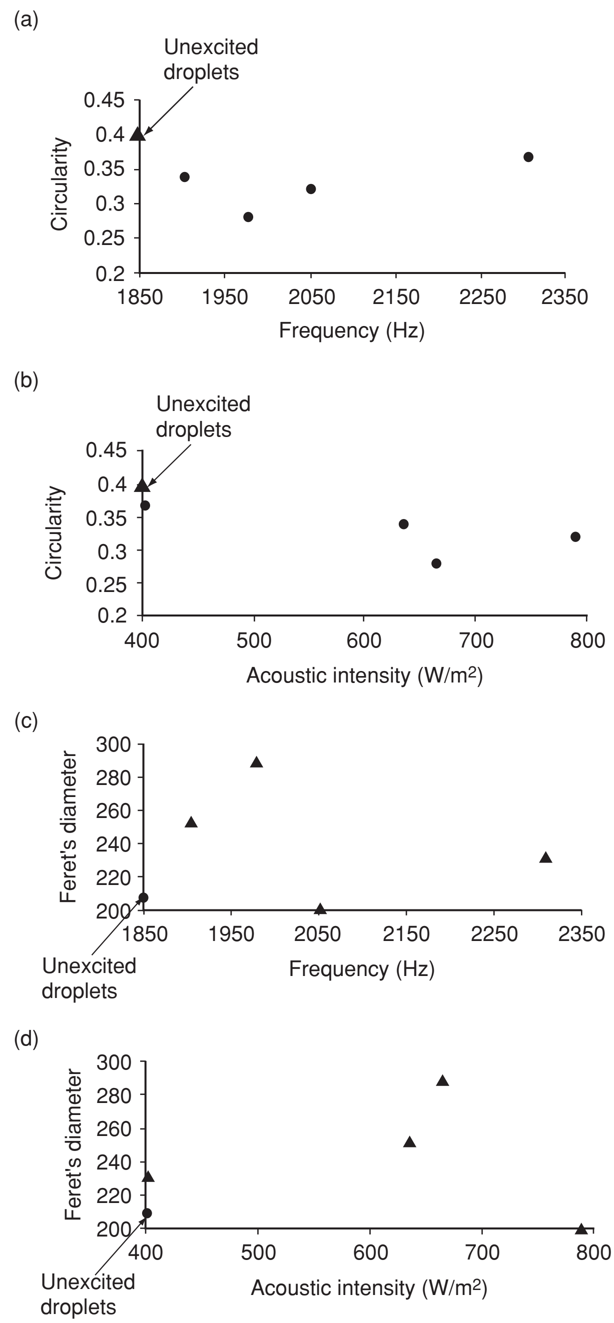

Figure 9: Variation of (a, b) Circularity, and (c, d) Feret's diameter of the droplet with acoustic frequency and acoustic intensity at $R = 4.92$, $L/D_j = 4.28$.

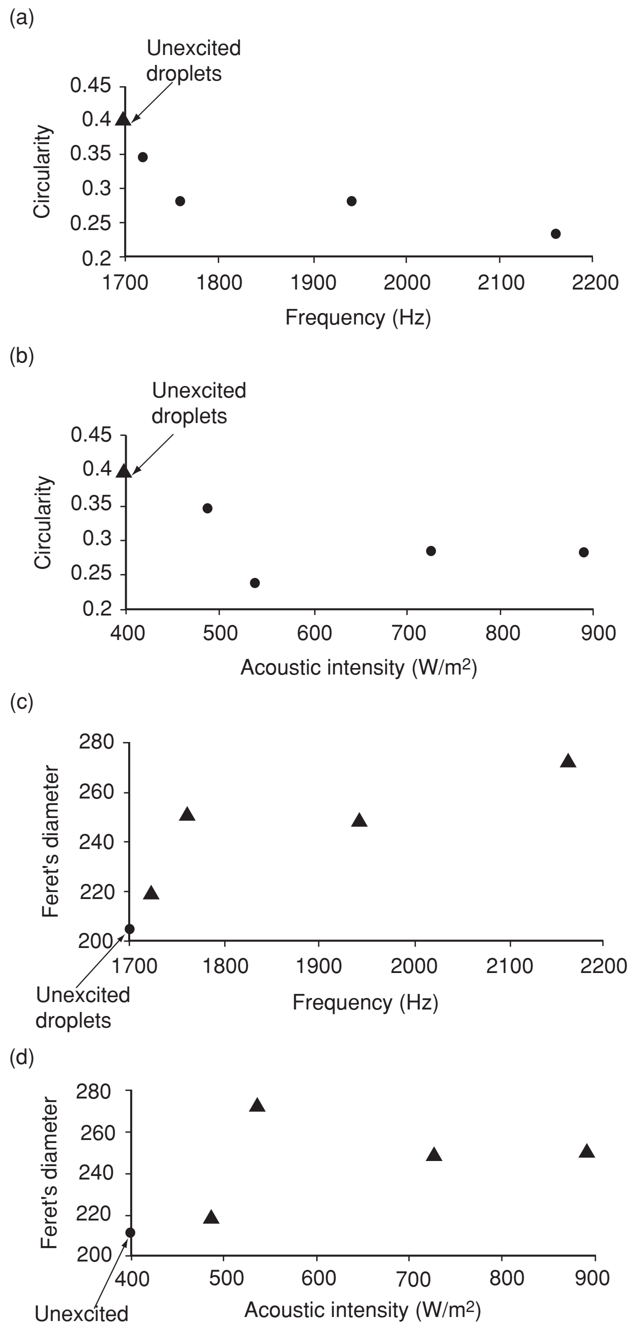

Figure 10: Variation of (a, b) Circularity, and (c, d) Feret's diameter of the droplet with acoustic frequency and acoustic intensity at $R = 5.91$, $L/D_j = 4.28$.

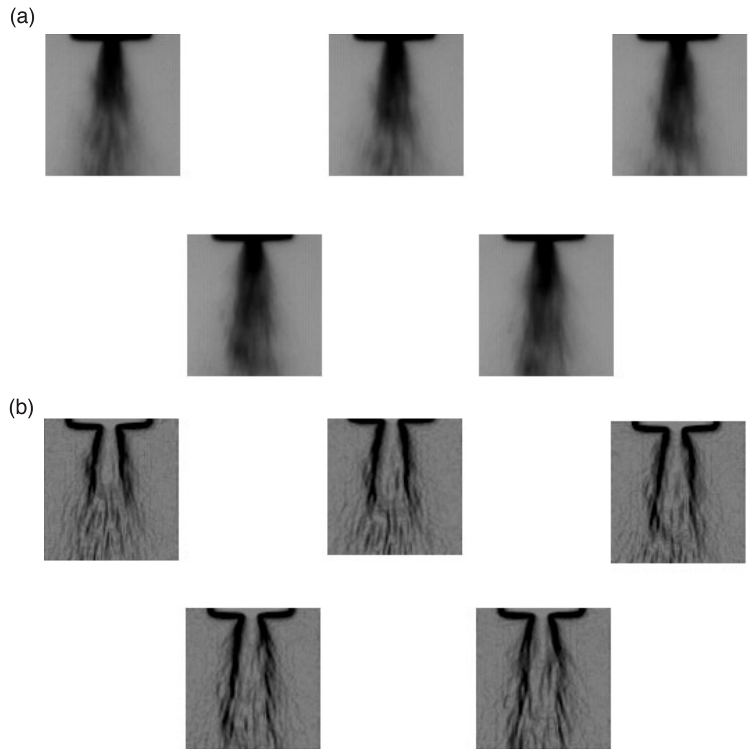

Figure 11: (a) Snapshots of raw image sequence of spray in the presence of acoustics, S/D_j = 2.86, L/D_j = 4.28, R = 5.91 at an ALR of 0.67%, (b) Edge detected image sequence of spray at the same conditions.

with time. In order to clearly understand the behavior of sprays further, the raw images of spray are averaged using the image analyzer “X-imager”, as mentioned earlier.

The average images of spray with and without acoustics at various ALR of 1.54%, 2.06%, and 2.66% are shown in Fig. 12. It is observed from the images that there is an increase in cone angle and width of the sprays in the presence of acoustics. The frequency (f) and sound intensity level (SIL) of Hartmann whistle at the injection location of sprays for different ALR values are mentioned along with Fig. 12.

The average spray images as well as its binary images for two different values of R are shown in Fig. 13, while maintaining the whistle parameters S/D_j = 2.86 and L/D_j = 4.28 constant. Cone angle of sprays increases in the presence of acoustics. The frequency (f) and sound intensity level (SIL) corresponding to the whistle parameters at the injection location for various ALR values are mentioned along with Fig. 13.

The variations in half cone angle of sprays with ALR, in the presence and absence of acoustics, are compared in Fig. 14 for two different S/D_j values. The half cone angle

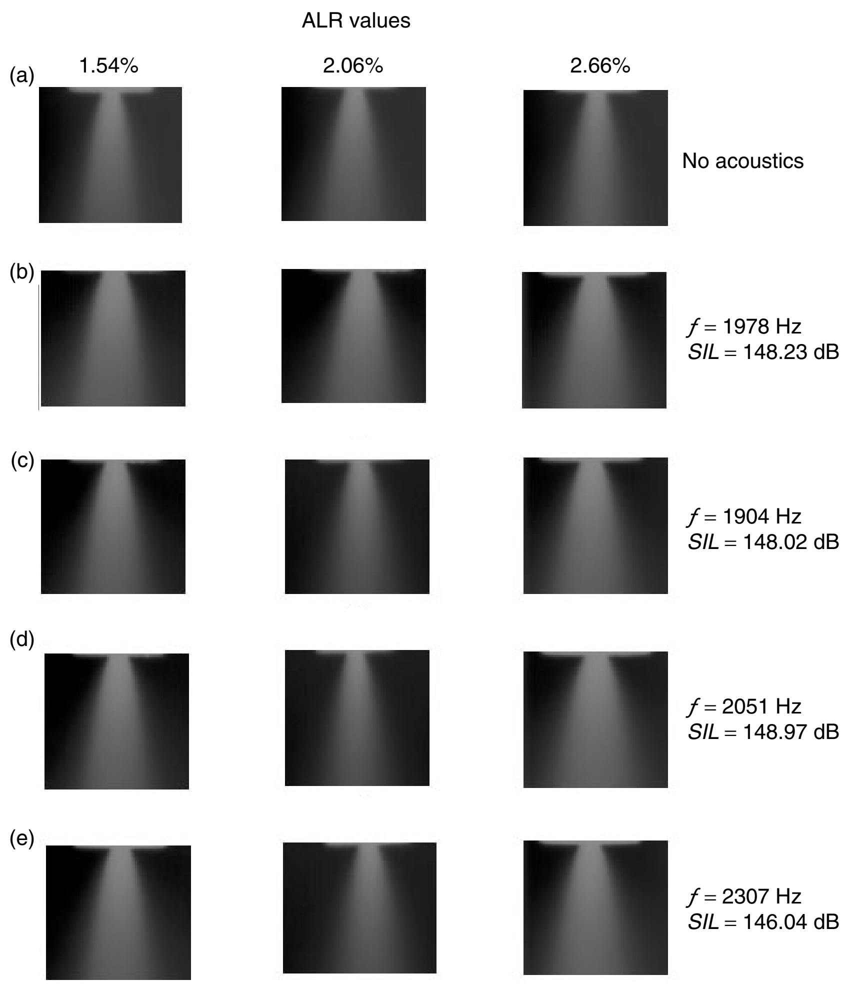

Figure 12: Average images of spray without and with acoustics, (a) without acoustics, with acoustics at $R = 4.92$, $L/D_j = 4.28$, for S/D_j values of (b) 2.86, (c) 3.28, (d) 4, (e) 4.57.

shows a monotonic increase with ALR for both cases (with and without acoustics). However, the half-cone angle values are higher in the presence of acoustics. Similar comparisons of half-cone angles are made in Fig. 15 for two different pressure ratios, for $S/D_j = 2.86$ and $L/D_j = 4.28$. The trends are similar, with acoustics augmenting the spray dispersion. However, no conclusion could be drawn about the effect of pressure ratio since the injection locations for the two cases were different (to avoid flow interference effects). From these results, it is clear that acoustic excitation plays a significant role in improving the atomization of sprays, quantified by the increase in

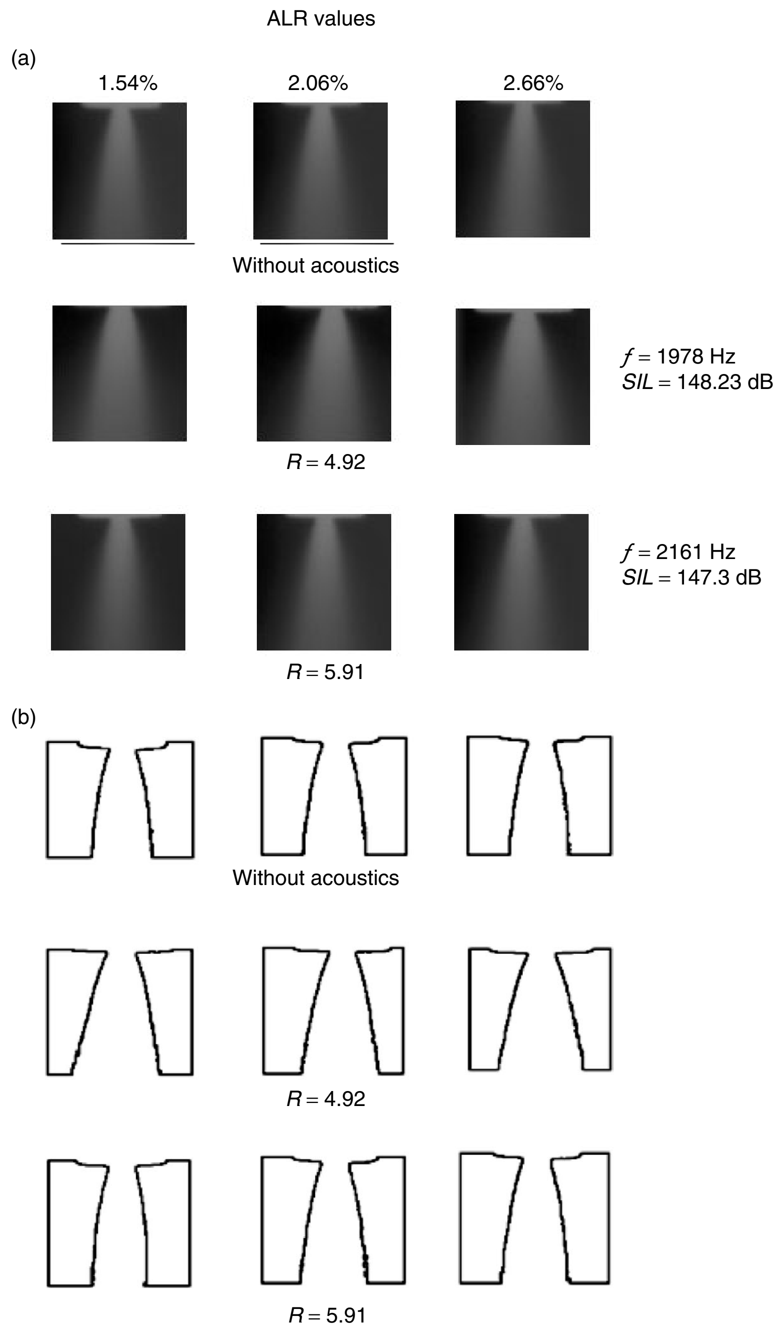

Figure 13: (a) Average spray images at S/D_j = 2.86 and L/D_j = 4.28 for different R, (b) Edge detected binary image for the same case.

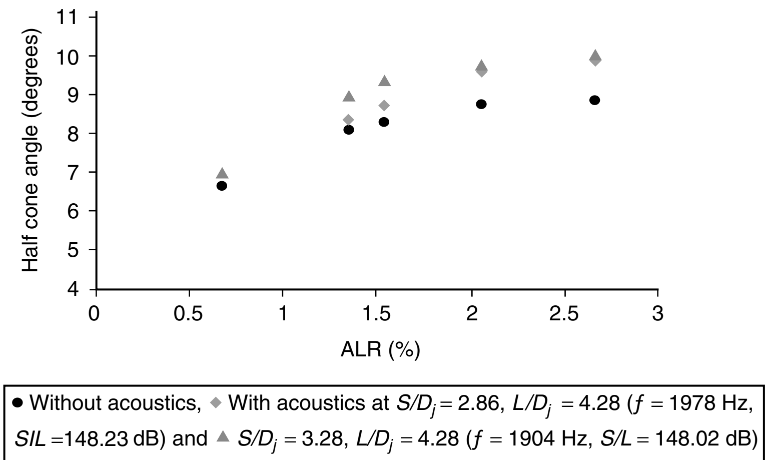

Figure 14: Variation of half spray cone angle with ALR, in the presence of acoustics at R = 4.92 and its comparison without acoustics.

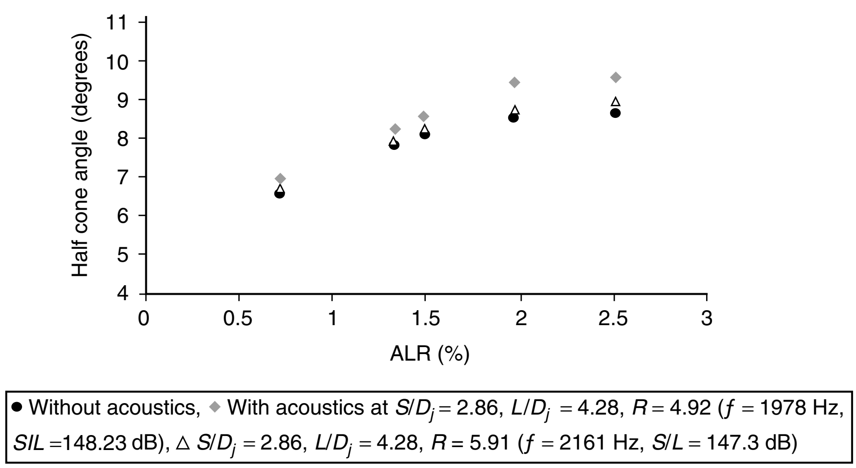

Figure 15: Variation of half spray cone angle with ALR, in the presence of acoustics (S/D_j = 2.86, L/D_j = 4.28) for R values of 4.92, and 5.91, and its comparison without acoustics.

cone-angles. The increase in cone angle of sprays is attributed to the fact that as the air bubbles emerge from the exit of the effervescent injector into large and directed sound field of Hartmann whistle, they undergo abrupt expansion and thus break the surrounding liquid into large number of fine droplets is probably due to enhanced entrainment of air into the spray due to its oscillations caused by the intense sound waves.

Figure 16 shows the half cone angle variation of the spray with Reynolds number. Reynolds number is calculated as

$$\mathrm{Re}_D = 4(\dot{m}_a + \dot{m}_w)/\pi D \mu_{mix} \tag{2}$$

where $\dot{m}_a$, $\dot{m}_w$ are the mass flow rates of the air and water, D is the spray jet diameter. μ_{mix} is the mass weighted average of the dynamic viscosity determined using the Eq. 3, where μ_a and μ_w are the dynamic viscosities of air and water respectively. It is seen that the half cone angle decreases with increase in Reynolds number showing that it has an inverse relation with ALR. The maximum cone angle is seen to be at a Reynolds number of around 8000.

$$\mu_{mix} = \frac{\dot{m}_a \mu_a + \dot{m}_w \mu_w}{\dot{m}_a + \dot{m}_w} \tag{3}$$

Figures 17 show the stroboscopic visualization of sprays for different whistle parameters. The edge detected image of sprays is also shown along with the raw images. Figure 17 (a) shows ligaments in sprays, which get scattered beyond a distance due to flow instabilities, in the absence of acoustics. However, the presence of acoustics causes the ligaments to break earlier, resulting in enhanced spreading [Fig. 17 (b)]. The excitation frequency (f) and the sound intensity level (SIL) corresponding to the whistle

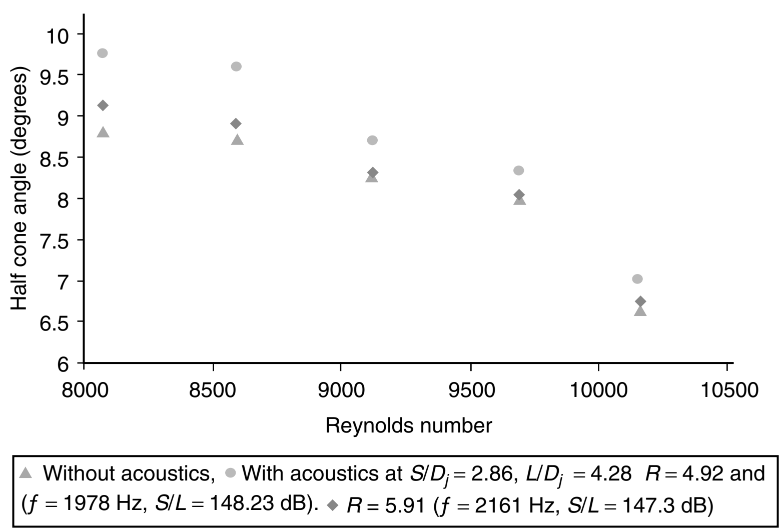

Figure 16: Variation of half spray cone angle with Reynolds number in the presence of acoustics (S/D_j = 2.86, L/D_j = 4.28) for R values of 4.92 and 5.91 and its comparison without acoustics.

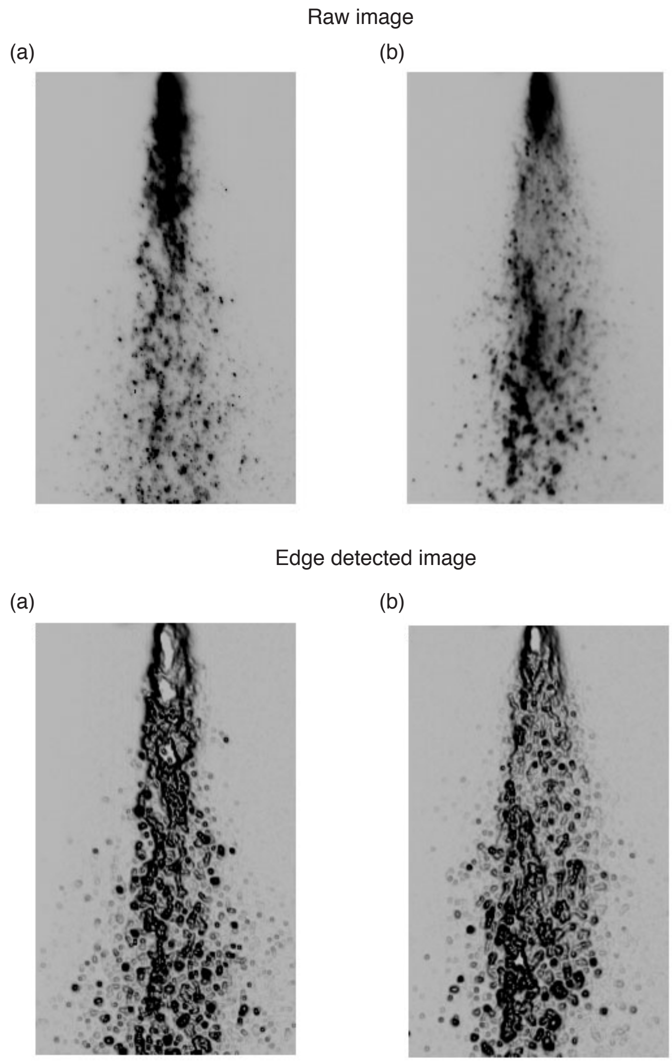

Figure 17: Stroboscopic visualization of sprays: water flow rate 1.5 *LPM*, air flow rate 10 *LPM*, (a) without acoustics, (b) with acoustics at S/D_j = 2.86, L/D_j = 4.28, R = 5.91 (f = 2161 Hz, SIL = 147.3 dB).

parameters at the injection location of sprays is also mentioned along with these Figs. Figure 18 represent the spray images at different water and air flow rates. Similar, features are observed at different ALR and acoustic excitation conditions. In this case, the extent of scattering in the presence of acoustics (Fig. 18 (b)) is observed to be high when compared to the previous case as shown in Fig. 17 (b).

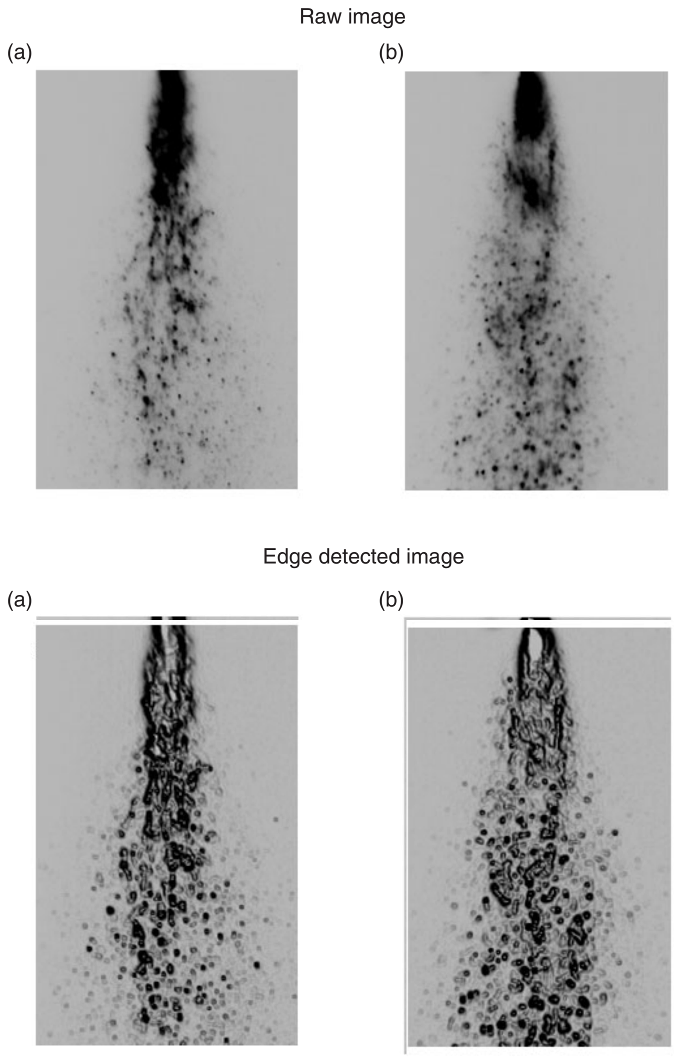

Figure 18: Stroboscopic visualization of sprays: water flow rate 1.33 *LPM*, air flow rate 15 *LPM*, (a) without acoustics, (b) with acoustics at S/D_j = 4, L/D_j = 4.28, R = 5.91. (f = 1758 Hz, SIL = 149.5 dB).

The comparison of sprays with (S/D_j = 2.86, L/D_j = 4.28, R = 4.92) and without-acoustics at an ALR of 1.378% is shown in Fig. 19 to represent the boundaries as well as the internal structure of sprays. The excitation frequency and sound intensity level in this case are 1978 Hz, 148.23 dB. The results clearly show increase in the number of droplets in the presence of acoustics in addition to larger spatial scattering of the

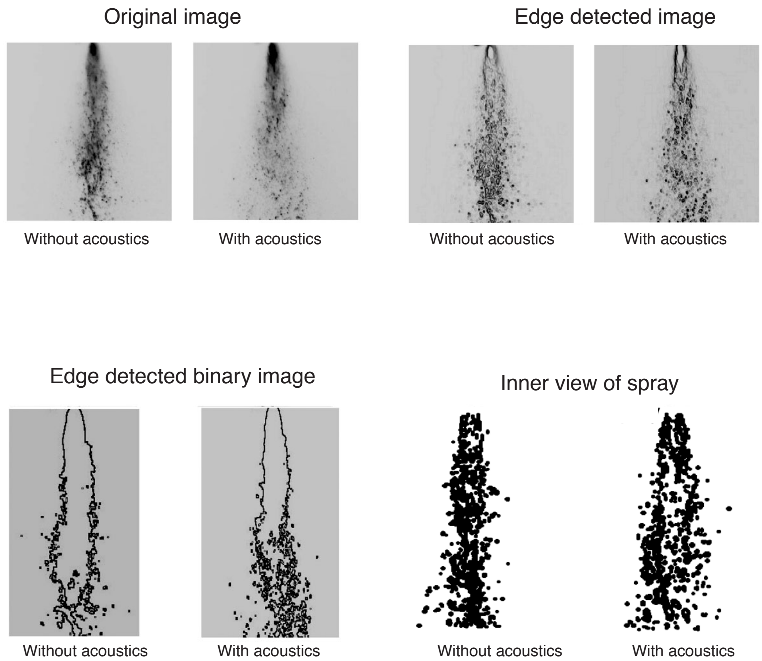

Figure 19: Comparison of spray images with acoustics at S/D_j = 2.86, L/D_j = 4.28, R = 4.92 and without acoustics, at an ALR of 1.378%.

droplets. The high intensity acoustic field causes large scatter of sprays and forms more number of droplets due to early break up of ligaments, thus changing its characteristics and is evident from the increase in cone angle. Thus the present studies clearly demonstrate the potential of acoustic excitation for atomization enhancement.

5. CONCLUSIONS

This paper explores the application of Hartmann whistle for atomization. For atomization studies, the effect of cavity acoustics is investigated on a single droplet first. Following this, the effect of acoustics on sprays is studied. The atomization studies on single droplet reveal that the presence of acoustic field causes the droplet to undergo large deformation and become irregular in shape. The extent of droplet deformation is quantified based on circularity and Feret's diameter. Smaller circularity and larger Feret's diameter indicates better deformation due to acoustics. The increase in half cone angle of spray to a higher value in the presence of acoustics in comparison to its absence shows that the acoustics enhances the atomization. The stroboscopic visualization of sprays in the presence of acoustics indicating an early break up of ligaments, large spreading as well as increase in the number of droplets shows atomization improvement.

ACKNOWLEDGEMENTS

The authors are grateful to Prof. R.I. Sujith for permission to use his image processing software "XIMAGER" for analysis of images in this work. The authors also gratefully acknowledge the funding from Indian Space Research Organization through the ISRO-IIT Madras Space Technology Cell, to carry out this work.

REFERENCES

[1] D. Danilov and M.A. Mironov, Breakup of a droplet in a high-intensity sound field, *Journal of the Acoustical society of America*, 1992, 92 (5), 2747–2755.

[2] M. Saito, M. Sato, and I. Suzuki, Evaporation and combustion of a single fuel droplet in acoustic fields, *Fuel*, 1994, 73 (3), 349–353.

[3] R.I. Sujith, G.A. Waldherr, J.I. Jagoda and B.T. Zinn, A theoretical investigation of the behavior of droplets in axial acoustic fields, *J. Vibration and Acoustics, Transactions of the American Society of Mechanical Engineers*, 1999, 121 (3), 286–294.

[4] I.F. Murray and S.D. Heister, On a droplet's response to acoustic excitation, *International journal of multiphase flow*, 1999, 25 (3), 531–550.

[5] M. Saito, M. Hoshikawa, and M. Sato, Enhacement of evaporation/combustion rate coefficient of a single fuel droplet by acoustic oscillation, *Fuel*, 1996, 75 (6), 669–674.

[6] A.I. Khandwawala, R. Natarajan and M.C. Gupta, Experimental investigation of liquid fuel atomization using Hartmann acoustic generator, *Fuel*, 1974, 53 (4), 268–273.

[7] K.M. Swamy, K.L. Narayana and J.S. Murty, Atomization of liquid fuels in an acoustic burner, *Fuel*, 1989, 68 (3), 387–390.

[8] R.K. Dubey, D.L. Black, M.Q. McQuay, and J.A. Carvalho, The effect of acoustics on an ethanol spray flame in a propane-fired pulse combustor, *Combustion and Flame*, 1997, 110 (1–2), 25–30.

[9] M.Q. McQuay, R.K. Dubey, and W.A. Nazeer, An experimental study on the impact of acoustics and spray quality on the emissions of CO and NO from an ethanol spray flame, *Fuel*, 1998, 77 (5), 425–435.

[10] R.L. Wilcox and R.W. Tate, Liquid atomization in a high intensity sound field, *American Institute of Chemical Engineers*, 1965, 11 (1), 69–72.

[11] R.I. Sujith, An experimental investigation of interaction of sprays with acoustic fields, *Experiments in Fluids*, 2005, 38 (5), 576–587.

[12] F. Barreras, H. Amaveda, and A. Lozano, Transient high-frequency ultrasonic water atomization, *Experiments in Fluids*, 2002, 33 (3), 405– 413.

[13] V. Sivadas, E.C. Fernandes and M.V. Heitor, Acoustically excited air-assisted liquid sheets, *Experiments in Fluids*, 2003, 34 (6), 736–743.

[14] J. Ju, Y. Yamagata, H. Ohmori and T. Higuchi, High-frequency surface acoustic wave atomizer, *Sensors and Actuators A*, 2008, 145–146, 437–441.

[15] K. Shuster, M. Fichman, A. Goldshtein and C. Gutfinger, Agglomeration of submicrometer particles in weak periodic shock waves, *Physics of Fluids*, 2002, 14 (5), 1802–1805.

[16] S. Narayanan, P. Bhave, K. Srinivasan, K. Ramamurthi, T. Sundararajan, Spectra and directivity of a Hartmann whistle, *J. Sound and Vibration*, 2009, 321, 875– 892.